Nuclear Medicine & Biology, Vol. 26, pp. 305–316, 1999

ISSN 0969-8051/99/$–see front matter
PII S0969-8051(98)00108-5

Evaluation of Gallium-68 Tris(2-Mercaptobenzyl)Amine: A Complex with Brain and Myocardial Uptake

Cathy S. Cutler,[1] M. Cecilia Giron,[1] David E. Reichert,[1] Abraham Z. Snyder,[1] Pilar Herrero,[1] Carolyn J. Anderson,[1] Duncan A. Quarless,[2] Stephen A. Koch[2] and Michael J. Welch[1]

[1]THE EDWARD MALLINCKRODT INSTITUTE OF RADIOLOGY, WASHINGTON UNIVERSITY SCHOOL OF MEDICINE, ST. LOUIS, MISSOURI, USA; AND [2]DEPARTMENT OF CHEMISTRY, STATE UNIVERSITY OF NEW YORK AT STONY BROOK, STONY BROOK, NEW YORK, USA

ABSTRACT. Previous research into development of a gallium-radiolabeled agent that crosses the blood–brain barrier has met with limited success. In this study, we focused our attention on a Ga(III) complex of a 4-coordinate amine trithiolate tripod ligand, tris(2-mercaptobenzyl) amine (S_3N). The Ga(III) S_3N complex is small, neutral, and lipophilic, meeting the requirements for a potential brain imaging agent. The Ga-68 complex was easily formed with a radiochemical purity of >95%. *In vitro* stability of the Ga-S_3N complex, determined in rat serum incubated at 37°C, was greater than 95% intact at 2 h by silica gel and reversed-phase radio-thin layer chromatography. Biodistribution studies conducted in female Sprague–Dawley rats showed the complex cleared rapidly from the blood with initial high liver uptake followed by rapid washout. Significant uptake was observed in the brain, with brain:blood ratios increasing from 0.11 at 2 min postinjection to 3.8 at 60 min postinjection. Uptake was also observed in the heart going from a heart:blood ratio of 2.3 at 2 min postinjection to 11 at 60 min postinjection. Molecular mechanics were used to determine the coordination number, and demonstrated that the Ga(III) complex prefers to be 4-coordinate. Imaging studies with ^{68}Ga-S_3N in a Nemestrina macaque showed significant brain uptake, similar to other lipophilic agents. The extraction of ^{68}Ga-S_3N into the brains of both rodents and primates, higher than any ^{68}Ga agent reported in the literature, suggests that this compound may have potential as a brain imaging agent for positron emission tomography. NUCL MED BIOL 26;3:305–316, 1999. **© 1999 Elsevier Science Inc. All rights reserved.**

KEY WORDS. Brain imaging agent, Ga(III), ^{68}Ga-S_3N, Heart imaging agent, Imaging

INTRODUCTION

Gallium-68 is a positron-emitting isotope with a half-life of 68 min and a high abundance of positrons (89%), making it ideal for positron emission tomography (PET) imaging. The half-life allows chemical manipulation but limits the dose received by the patient. Unlike many of the other isotopes used for PET that are cyclotron produced, ^{68}Ga is obtained from a ^{68}Ge/^{68}Ga generator. Germanium-68 ($t_{1/2}$ = 280 days) is loaded onto a tin dioxide column, which decays by electron capture to ^{68}Ga (20). The generator can be eluted several times a day with 1 N HCl, producing ^{68}Ga in a form suitable for rapid synthesis of radiopharmaceuticals. The long half-life of the ^{68}Ge parent (280 days) allows for a shelf-life of 1.5–2 years for the generator (2). This generator system enables hospitals that are unable to afford the expense of a cyclotron to perform PET imaging.

Several requirements must be met to design appropriate radiopharmaceuticals for heart and brain imaging. Work at Washington University has shown the usefulness of lipophilic ethers and alcohols labeled with ^{11}C ($t_{1/2}$ = 20 min) for measurement of myocardial and cerebral blood flow by PET (4, 12). High spin Fe and Ga, due to their similar electronic configuration (Fe^{3+} = $3d^5$, Ga^{3+} = $3d^{10}$), have many common properties, including ionic radii (Fe^{3+} = 0.49 Å, Ga^{3+} = 0.47 Å), ionization potential, and coordination number. A major problem encountered with gallium radiopharmaceuticals is the transchelation of Ga(III) to various iron-containing proteins (particularly transferrin), which bind Ga(III) with high affinity (17). The radiopharmaceuticals ^{67}Ga- and ^{68}Ga-citrate actually take advantage of this transchelation by labeling transferrin *in vivo* by ligand exchange; ^{68}Ga-transferrin measures regional plasma volume and ^{67}Ga-transferrin is used as a diagnostic agent for infection and neoplasms. Perfusion imaging necessitates high stability Ga(III) radiopharmaceuticals that will not undergo transchelation with transferrin. For brain imaging, the compound must be relatively small, neutral, and lipophilic to cross the intact blood–brain barrier.

Several gallium agents have been developed that show significant myocardial uptake. Green and co-workers developed a series of uncharged lipophilic Ga(III) complexes of 1,1,1-tris-(5-methoxy-salicylaldiminomethyl)ethane [$(sal)_3$tame] and 1,1,1,-tris-(alkoxy-salicylaldiminomethyl)ethane derivatives [$(ROsal)_3$tame] as ^{68}Ga myocardial imaging agents (8, 11). In an attempt to increase heart uptake, the lipophilicity of these ligands was further increased by the addition of alkoxy-substituents on the ethane backbone of the triamine framework of the tris(salicylaldimine) ligands. Increased heart uptake and higher heart:blood ratios were observed. However, the increased lipophilicity resulted in increased liver accumulation (10). Gallium(III) complexes of bis-aminoethanethiol-cyclohexyl

Address correspondence to: Michael J. Welch, Ph.D., Washington University School of Medicine, Division of Radiological Sciences, 510 S. Kingshighway, Box 8225, St. Louis, MO 63110, USA; e-mail: welch@mirlink.wustl.edu.

Received 1 November 1998.
Accepted 20 November 1998.

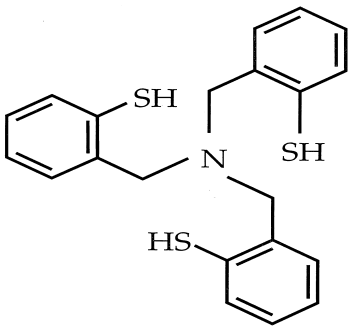

FIG. 1. Structure of tris (2-mercaptobenzyl) amine (S_3N).

(BAT-TECH) ligands have been investigated as possible myocardial imaging agents (6, 19). The Ga(III) compounds are taken up rapidly by the heart; however, they wash out quickly and the blood level remains high, resulting in low heart:blood ratios at later time points. In an attempt to design myocardial imaging agents with increased myocardial retention, Tsang and co-workers prepared a series of hexadentate bis(salicylaldimine) ligands that formed lipophilic cationic complexes with Ga(III) (37, 38). These compounds, particularly Ga(III)[(4,6-MeO_2sal)$_2$BAPEN]$^+$, exhibited significant myocardial uptake, with longer retention than any of the compounds mentioned previously.

Investigations into developing a Ga(III) brain agent has met with limited success. A series of tris(1-aryl-3-hydroxy-4-pyridinonato) Ga(III) complexes exhibited liver and heart uptake in rats and dogs. One complex, 3-hydroxy-2-methyl-1-(*p*-nitrophenyl)-4-pyridinone labeled with Ga(III), by planar imaging of normal rabbits showed brain accumulation, which increased over time (39). However, a biodistribution of the same complex in normal Wistar rats showed no brain accumulation. Because the uptake was observed only by planar imaging, it is not clear if the activity was definitely located in the brain or in some other tissue such as the skull. ^{68}Ga-[*N,N,N',N'*-tetrakis-(2-hydroxy-3,5-dimethylbenzyl)ethylenediamine], a neutral lipophilic hexachelated compound, exhibited significant myocardial uptake; however, the brain uptake was insufficient to allow for measurement of cerebral blood flow (21).

Previous work performed in our group has shown that Ga(III) forms stable complexes with either 4-, 5-, or 6-coordinate ligands, with 6-coordinate being the most stable (34). In our attempts to develop a Ga-68 imaging agent to cross the blood–brain barrier, we focused our attention on a 4-coordinate amine trithiolate tripod ligand, tris(2-mercaptobenzyl) amine (S_3N), shown in Figure 1. Designed by Koch and co-workers to study the electronic and structural characteristics of metalloproteins and enzymes containing Fe(II) and Fe(III) (7), the Fe(III) S_3N complex was relatively small, lipophilic, and neutral, making it intriguing as a possible brain agent with Ga(III).

Computational methods provide a means for understanding structure and its relation to function. Thus the development of force fields and techniques for modeling radiometal complexes provide tools for the design of new imaging and therapeutic agents with enhanced properties. Previous modeling studies have evaluated 4-, 5-, and 6-coordinate Ga(III) and In(III) complexes (34), Tc(V) oxo complexes (16), and gadolinium-based magnetic resonance imaging (MRI) contrast agents (28).

In this paper, we present the preparation and *in vivo* evaluation of ^{68}Ga-labeled S_3N. ^{68}Ga-S_3N was evaluated in normal rats and hamsters and used to image a nonhuman primate and a canine. The brain distribution of ^{68}Ga-S_3N was further characterized by autoradiography studies and compared to two well-studied perfusion tracers, ^{11}C-ethanol (4) and ^{64}Cu-pyruvaldehyde bis(N^4-methylthiosemicarbazone) (PTSM) (9).

EXPERIMENTAL

Materials and Methods

RADIOCHEMISTRY. S_3N was prepared by methods reported previously (7). All materials were reagent grade unless otherwise specified. $^{68}GaCl_3$ was obtained from a 25 mCi ^{68}Ge/^{68}Ga generator (Dupont Pharma, N. Billerica, MA). Water was distilled and then deionized (18 MΩ/cm^2) by passing through a Milli-Q® water filtration system (Millipore Corp., Bedford, MA). C-18 Sep-Pak® Light cartridges were purchased from Waters Corporation (Milford, MA). Sodium acetate was obtained from Fluka Chemie AG (Buchs, Switzerland). Diethylenetriaminepentaacetic acid (DTPA) was purchased from Sigma Chemical Co. (St. Louis, MO).

High performance liquid chromatography (HPLC) analysis was carried out on a Scientific Systems, Inc. HPLC system (SSI, State College, PA), with an Alltech C18 10 μ Versapack 300 $\times$ 4.4 mm column (Alltech Associates, Deerfield, IL). The gradient mobile phase was started at 65% B and increased to 80% B over 20 min (A = water, B = acetonitrile) at a flow rate of 1 mL/min. Sequential radiometric detection with a Beckman model 170 Radioisotope detector (Fullerton, CA) was followed by ultraviolet (UV) detection with a Linear Variable Wavelength UV/VIS 204 detector (Linear Instruments Corp., Reno, NV) or a SSI model 500 Variable Wavelength detector operating at 254 nm. SSI Vision IV software was used to integrate the chromatograms. Silica gel thin layer chromatography (TLC) plates (60 Å, F254) were obtained from P.J. Cobert (St. Louis, MO) and Waters C18 silica gel TLC plates (KC18F, 60 Å, 200 μm) were purchased from Fisher Scientific (Pittsburgh, PA). Radio-TLC chromatograms were analyzed on either a Bioscan 200 imaging scanner (Bioscan, Inc., Washington DC) or a Berthold Automatic TLC-Linear Analyzer (Berthold System, Inc., Pittsburgh, PA). Radioactivity was counted with a Beckman Gamma 8000 counter containing a NaI crystal (Beckman Instruments Inc., Irvine, CA). Autoradiography experiments were performed on a Packard Instant Imager Electronic Autoradiography System (Packard Instrument Company, Meriden, CT). $^{64}CuCl_2$ was prepared at Washington University using a biomedical cyclotron as described previously (25).

Complex charge was determined by electrophoresis with a Helena Laboratories electrophoresis chamber (Beaumont, TX) using Sepraphore III cellulose polyacetate strips (Gelman Sciences Inc., Ann Arbor, MI) presoaked in 0.1 M sodium acetate buffer, pH 7.4, and run with a Bio-Rad model 1000/500 power supply (Richmond, CA) at a constant current of 8 mA and a voltage of 250 mV for 45 min. ^{111}In-DTPA, known to have an overall charge of -2, was used as a standard. The strips were analyzed by the Bioscan 200 imaging scanner to determine the migration of radioactivity and overall charge of the complex.

PREPARATION OF RADIOACTIVE COMPOUNDS. The ligand solution was prepared by dissolving ~1 mg of ligand in 1 mL of ethanol that had been degassed for 15 min with argon. $^{68}GaCl_3$ (15–20 mCi) was eluted from the ^{68}Ge/^{68}Ga generator with 3 mL of 1 N HCl. The $^{68}GaCl_3$ was evaporated to dryness with a heat gun under a stream of nitrogen, redissolved in 1 mL of ethanol, and degassed for 10 min with argon. The ligand solution (100 μg; 80–120 μL) was then added to the dried $^{68}GaCl_3$ and incubated at room temperature for 10 min. Quality control was determined by radio-TLC on C18

plates developed in 90% methanol:10% water, and by radio-TLC on silica plates developed in 100% methanol.

The product was purified by addition of 3 mL of saline and subsequent loading onto a preconditioned C18 Sep-Pak Light (prepared by washing with 3–5 mL of ethanol, followed by 3–5 mL of normal saline) to remove excess ligand and uncomplexed ^{68}Ga. The Sep-Pak was then washed with 3 mL of saline. The complex was eluted with 400 μL of ethanol. Saline was then added to the eluent to give a resultant solution of 85% saline/15% ethanol and the percentage complex was determined by TLC.

Complex charge was determined by the electrophoresis procedure described above. ^{64}Cu-PTSM was prepared and analyzed as described previously (23), with the exception that PTSM was dissolved in dimethyl sulfoxide (DMSO) rather than ethanol.

In a separate experiment, a previously published procedure for the preparation of alkyl iodides was adapted to synthesize ^{11}C-ethanol (4). Briefly, ^{11}C-CO_2 was bubbled through 1.0 mL dry ether containing 50–70 μL of 3 M methylmagnesium bromide, followed by addition of 200 μL of 1 M lithium aluminum hydride and 200 μL of ether. The mixture was then heated at 100°C for 3 min. The solvent was evaporated and 1.0 mL of 1.0 N HCl was added to decompose the lithium complex. ^{11}C-ethanol was distilled at 90–95°C with a stream of nitrogen and collected in 1.5 mL of saline.

DETERMINATION OF PARTITION COEFFICIENTS. The partition coefficients (log P; n = 3) were determined by adding 5–20 μL of labeled complex to a solution containing 2 mL of octanol and 2 mL of water (obtained from saturated octanol water solutions). The resulting solutions were then vortexed and centrifuged for 5 min at 2,400 rpm. Octanol (1 mL) was removed and back extracted with 1 mL of water, vortexed, and centrifuged as before. Octanol (500 μL) and water (500 μL) were removed and counted. Water (500 μL) was added to the 500 μL of octanol, vortexed, and centrifuged as before. Aliquots (200 μL) of octanol and water were removed and counted. The partition coefficent was calculated as a ratio of counts in the octanol fraction to counts in the water fraction per extraction. The average log P value of the two back extractions is reported.

SERUM STABILITY STUDIES. *In vitro* serum stability studies were conducted by placing 100 μCi of ^{68}Ga-S_3N in 500–1,000 μL of freshly drawn rat serum and incubating at 37°C. Samples were removed at various time points and analyzed by both the C18 and silica radio-TLC procedures listed above. *In vivo* stability studies involved the injection of 500–1,000 μCi of ^{68}Ga-S_3N into the tail vein of mature female Sprague–Dawley rats (Sasco, Omaha, NE). Blood samples were removed via cardiac puncture (200–250 μL) at various times postinjection. Ethanol was then added (800–1,000 μL) and the entire solution vortexed and centrifuged at 14,000 rpm for 5–6 min on the Eppendorf 5415 Centrifuge to separate the supernatant from the residual proteins. The supernatant was then decanted, counted, and analyzed by radio-TLC methods listed previously. Controls consisted of radiolabeled compound added directly to freshly drawn blood and then treated the same as above. Figure 2 presents data as percent authentic intact. The percent authentic intact is calculated using an equation that takes into consideration the purity of the injectate, the percent of activity extracted from the organ, percent of intact complex determined by radio-TLC, and the percent extraction of the controls.

BIODISTRIBUTION STUDIES. All animal studies were performed in compliance with guidelines set forth by the Washington University Animal Studies Committee. Mature female Sprague–Dawley rats (n = 4 per time point) weighing 150–200 g were anesthetized with Metofane (2, 2-dichloro-1, 1-difluoro-1-methoxyethanol) and injected with 15–20 μCi of ^{68}Ga-S_3N in a volume of 150–200 μL 85% saline/15% ethanol via the tail vein. The rats were anesthetized prior to sacrifice (by decapitation) at each time point. The lung, liver, spleen, kidney, heart, and brain were removed from each animal, placed on absorbent paper, and weighed. Blood samples were collected directly and weighed. Blanks and standards were prepared and counted along with the samples, to calculate the percent injected dose per gram of tissue (%ID/g) and percent injected dose per organ (%ID/organ), and to correct for physical decay.

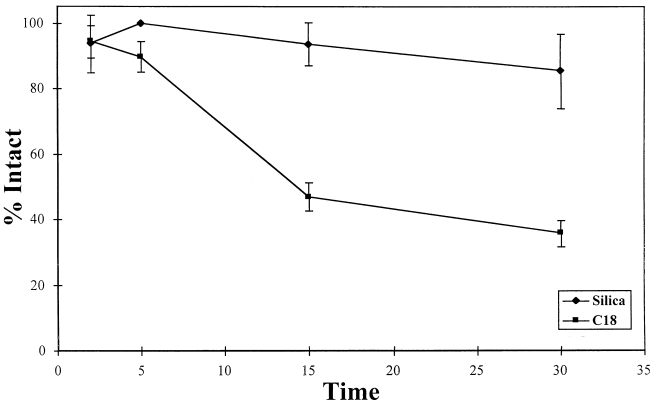

FIG. 2. Graph of the *in vivo* stability of ^{68}Ga-S_3N over time. The percentage of the intact complex as determined by both silica and reversed phase thin layer chromatography (TLC) at various time points postinjection.

A biodistribution study of female Golden Syrian hamsters (Charles River Laboratories, Wilmington, MA) weighing 100–120 g (n = 4 per time point) was carried out similarly to the rat biodistribution, except 14 μCi of ^{68}Ga-S_3N in 100 μL of 85% saline: 15% ethanol were injected intracardially.

AUTORADIOGRAPHY EXPERIMENTS. Mature female Sprague–Dawley rats were injected with approximately 400 μCi of ^{68}Ga-S_3N and 47 μCi of ^{64}Cu-PTSM as a regional perfusion marker (30, 31) via the tail vein, anesthetized, and sacrificed at 30 min postinjection. The brain was removed, frozen, and cut into 1-mm thick slices with a gauged slicer, and Ga-68 images were obtained on the Instant Imager. After decay of Ga-68, Cu-64 images were obtained with the Instant Imager.

In a separate experiment, 180–200 μCi (200 μL) of ^{11}C-ethanol were injected via the tail vein into an anesthetized rat, and the rat was then sacrificed at 1 min postinjection. The brain was removed and prepared as above and imaging was performed on the Instant Imager.

PRIMATE IMAGING STUDY. A male Nemestrina monkey weighing 16 kg was anesthetized with 300 mg of ketamine, 10 mg of xylazine, and 0.2 mg of atropine sulfate injected intramuscularly. The animal was injected with 25 mCi of O-15-labeled water to measure brain blood flow and 20 mCi of carbon monoxide was administered by inhalation to determine blood volume. ^{68}Ga-S_3N (3.4 mCi) was administered intravenously (IV). One-minute images were acquired for 15 min and then 19 5-min images acquired, for a total acquisiton time of 110 min. PET imaging studies were performed on a 953B PET scanner in the two-dimensional mode. The reconstructed

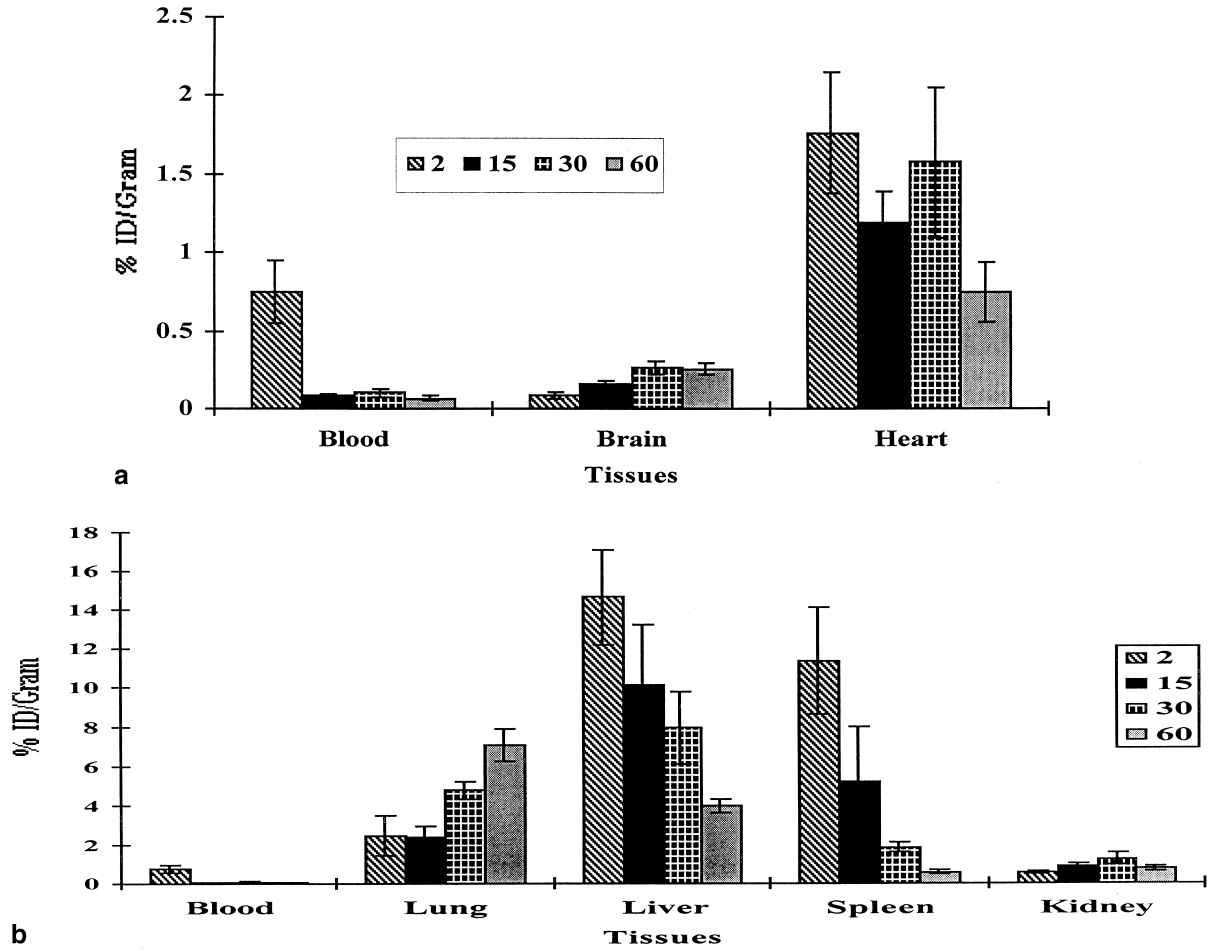

FIG. 3. Graph of the biodistribution of ^{68}Ga-S_3N in normal Sprague–Dawley rats at 2, 15, and 30 min and 1 h postinjection. (a) Comparison of the percent injected dose per gram of tissue (%ID/g) obtained in the blood, heart, and brain. (b) Comparison of the %ID/g observed in the blood, lung, liver, spleen, and kidney.

resolution was approximately 6 mm in the transverse plane and about 4.5 mm in the axial direction; axial sampling was about 3.4 mm (24, 32, 33). The animal was fasted overnight prior to the study but allowed free access to water up to 2 h before the study. MRI studies utilizing a Siemens Vision 1.5 Tesla Imager was performed with the animal fully anesthetized. Careful monitoring of the animal's condition including temperature, end-tidal CO_2, respiratory rate, electrocardiogram, and pulse provided online information during the MRI scans. There were no signs of distress throughout the PET or MRI procedure.

CANINE IMAGING STUDY. An adult male canine weighing 27 kg was premedicated with 0.75 mg atropine and 5 mg of acepromazine subcutaneously. After 30 min, anesthesia was induced with 12.5 mL 5% sodium thiopental given IV via an established right cephalic vein catheter. The animal was intubated with a 9 french endotracheal tube and ventilated mechanically (tidal volume =15 mL/kg) on an Ohio 30/70 proportioned anesthesia machine using 1.5–2.5% inhalant isoflurane. Anesthesia was maintained throughout the procedure. The animal was injected with 21 mCi of O-15-labeled water and 22 mCi of carbon monoxide. ^{68}Ga-S_3N (5.97 mCi) was injected through the established right cephalic vein IV line. Imaging was performed on the 953B scanner as discussed above; acquisitions were acquired for 5 min for a total of 90 min.

Molecular Modeling

DETERMINATION OF THE COORDINATION NUMBER. Hancock and co-workers have utilized molecular mechanics successfully to determine the relationship between ligand selectivity and metal ion size (13–15, 35). The technique utilized in these studies was the calculation of the complex strain energy as a function of the M-L bond length. A related technique is the "coordination scan," in which a series of energy curves are generated by minimizing strain energy of complexes with various numbers of coordinated water molecules and M-L bond lengths (18). The preferred coordination number of the metal is determined by the position of the ionic radius (29) in relation to the intersection points of the energy curves. This technique has previously been found to successfully predict the coordination number of various Ga(III) and In(III) complexes (34).

The coordination scan technique was used to determine the coordination number of the Ga(III) S_3N complex. The starting structure was that of the previously reported Fe(III) x-ray coordinates (7). The metal in each complex was then adjusted to the different coordination numbers by covalently binding the appropriate number of waters to the metal. An important point to note is that the modeling package SYBYL (36) calculates water as having

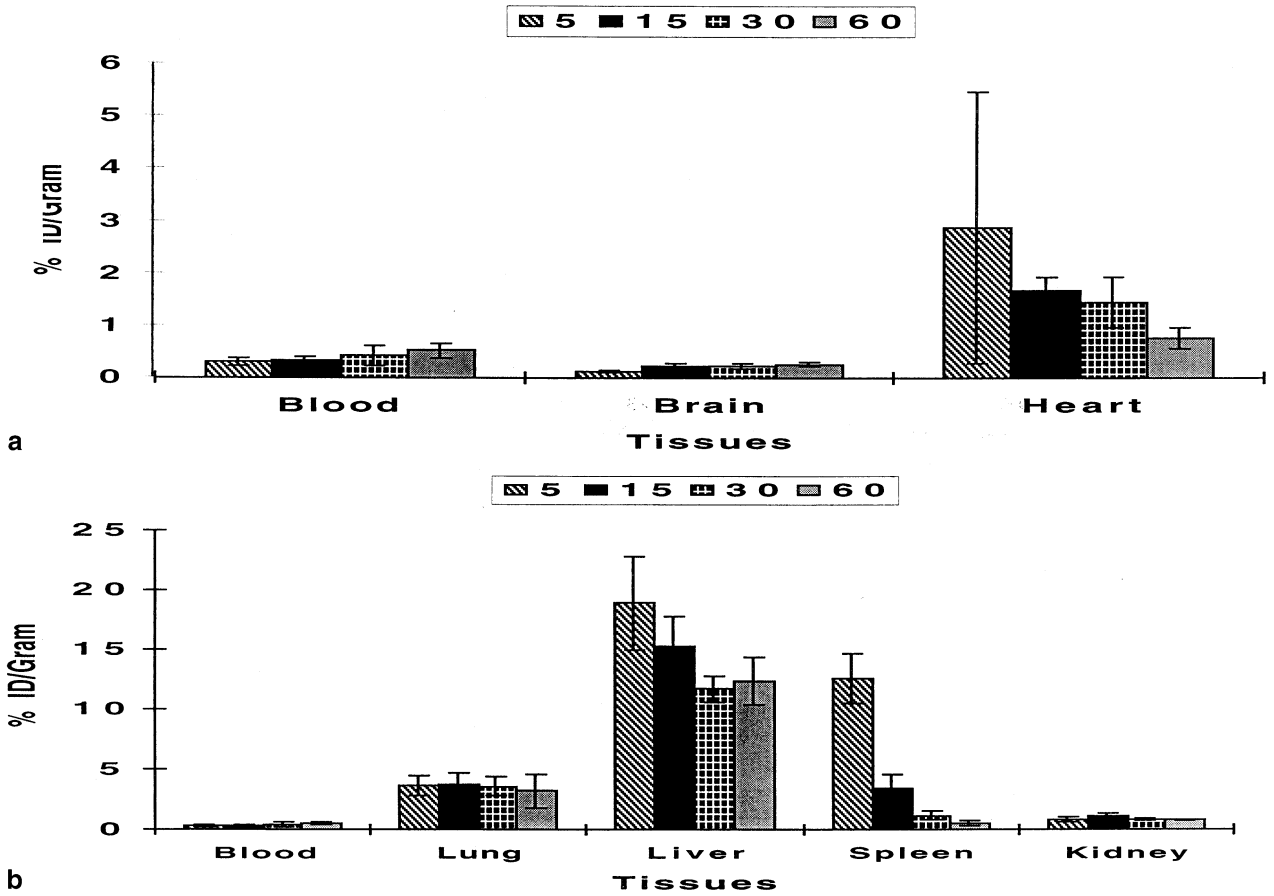

FIG. 4. Graph of the biodistribution of ^{68}Ga-S_3N in normal Golden Syrian hamsters at 5, 15, and 30 min and 1 h postinjection. (a) Comparison of the percent injected dose per gram of tissue (%ID/g) obtained in the blood, heart, and brain. (b) Comparison of the %ID/g observed in the blood, lung, liver, spleen, and kidney.

a strain energy of 0.00 kcal/mol, thus the waters added to the complex add no energy other than steric interactions with the ligand.

Force field parameters for bonds between N, O, and S donor atoms with Ga(III) were those developed for the modeling package SYBYL (36), and utilized in a study of *N,N′*-ethylene-di-L-cysteine (EC) complexes (1). The metal's ionic radius was effectively varied by systematically altering the M-N, M-S, and M-O equilibrium bond lengths in the following manner. The M-N bond length was assigned through the following relationship: eq. bond length = (M ionic radius) + 1.58 Å. Similarly, the M-O equilibrium bond lengths were assigned using: eq. bond length = (M ionic radius) + 1.41 Å. The M-S equilibrium bond lengths were assigned using: eq. bond length = (M ionic radius) + 1.76 Å. The initial metal ionic radius was set to 0.3 Å. The force constant for the bond stretching was kept at a constant value of 100 kcal mol^{-1} $Å^{-1}$. The complex was then minimized using this ionic radius, and the energy of the complex found. The ionic radius was then increased by 0.1 Å, the equilibrium bond length modified to the new value, and the complex again minimized. This process was continued until the ionic radius had reached 1.5 Å; this range of 0.3–1.5 Å was sufficiently large that it covered the radii of all the possible coordination states. This procedure was then repeated for the complex with one water, two waters, and so on, until all the possible coordination states were examined.

Plots of the complex energy versus metal ionic radius were then generated for each coordination number. The preferred coordination number of a metal is found by locating the preferred ionic radius on the x-axis of the plot and the lowest energy curve, which corresponds to the preferred coordination number. For Ga(III), the radius for a 4-coordinate environment is 0.47 Å; for 5-coordinate, the radius is 0.55 Å; and for 6-coordinate, the radius is 0.62 Å.

RESULTS

Radiochemistry

The radiochemical yield of ^{68}Ga-S_3N was consistently >95%. ^{68}Ga-S_3N migrated with an R_f = 0.8 on silica plates developed in 100% methanol and an R_f = 0.4 on C18 plates developed in 90% methanol:10 % water (v/v). In both systems, $^{68}GaCl_3$ remained at the origin.

In electrophoresis experiments, the ^{68}Ga-S_3N complex migrated with an R_f = −0.01. The standard ^{111}In-DTPA migrated with an R_f = 0.24. These results indicate that the ^{68}Ga-labeled S_3N complex was neutral.

The octanol-water partition coefficient or log P of ^{68}Ga-S_3N was determined to be 1.8 ± 0.1. Dischino and co-workers (4) studied the relationship between the lipophilicity of a compound and its extraction by the brain. Their results showed that a radiopharmaceutical designed to measure blood flow should have a log P value

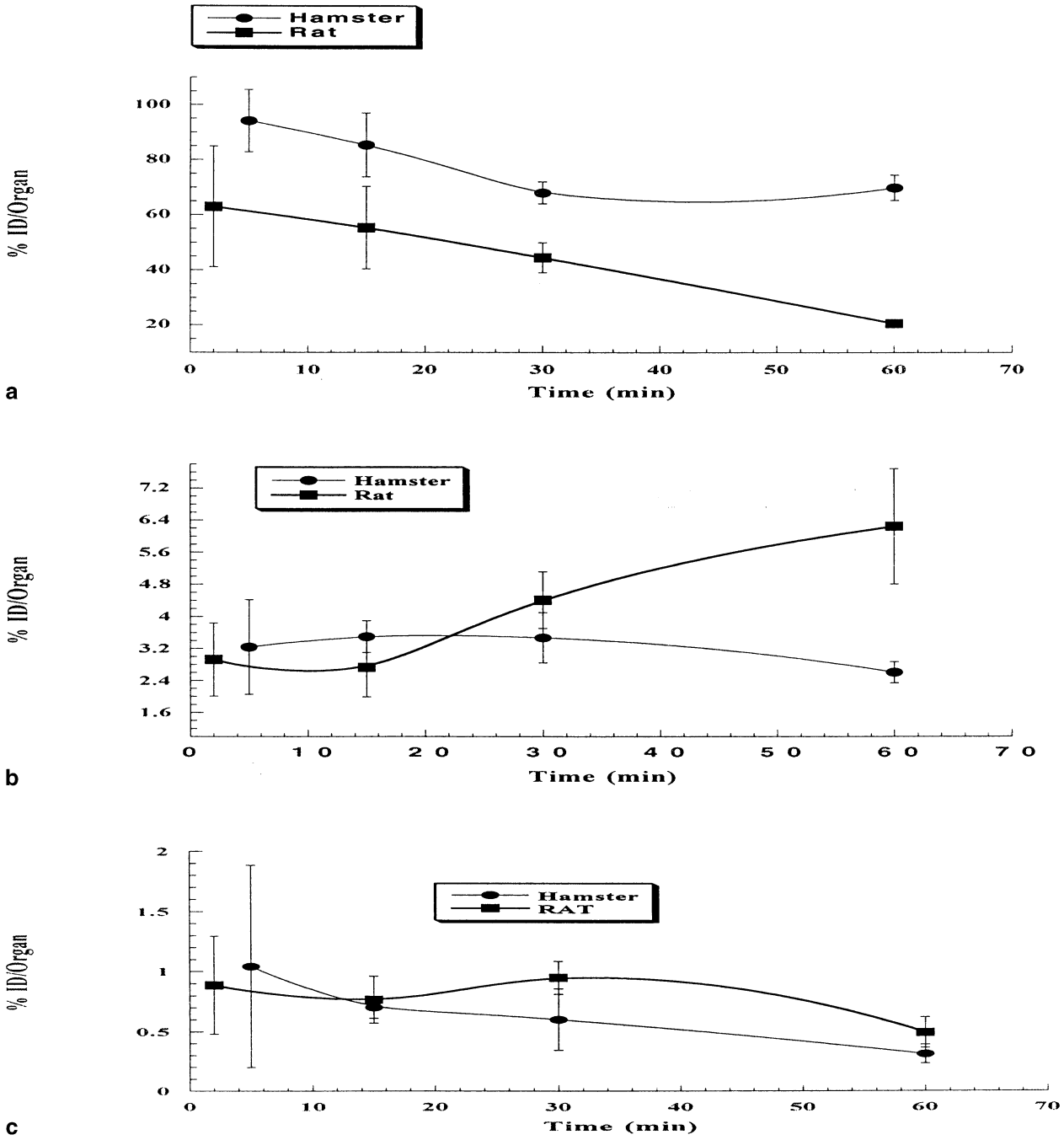

FIG. 5. Graphs comparing the percent injected dose per organ (%ID/organ) of uptake in normal hamsters and rats. (a) Comparison of the clearance observed in the liver. (b) Comparison of the lung uptake over time. (c) Comparison of heart uptake.

of between 0.9 and 2.5 (4). Based on these results, the log P value of 1.8 ± 0.1 obtained for ^{68}Ga-S_3N is right in the middle of the range suggested by Dischino and therefore should freely diffuse across the blood–brain barrier.

Serum Stability

The *in vitro* stability of ^{68}Ga-S_3N remains more than 95% intact up to 2 h. The *in vivo* stability results of ^{68}Ga-S_3N, determined by both silica and C18 TLC, are shown in Figure 2. The intact complex and metabolites migrate with the same R_f on silica gel TLC, therefore it is only resolving complexed gallium from uncomplexed gallium. The metabolites, intact complex and uncomplexed gallium, are resolvable by C18 TLC. ^{68}Ga-S_3N remains more than 93% intact at 2 min. At 5 min, 90% remains intact with the remaining activity attributed to a less lipophilic metabolite. By 30 min, the percent authentic intact dropped to 36%, with the remaining activity comprised largely of the metabolite observed at 5 min and a small amount of an even less lipophilic metabolite.

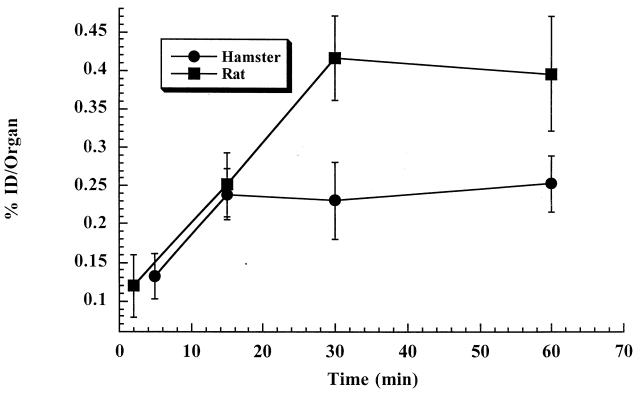

FIG. 6. Graph comparing the hamster and rat brain uptake observed for ^{68}Ga-S_3N (percent injected dose per organ [%ID/organ]).

Biodistribution Experiments

The biodistribution results in rats for ^{68}Ga-S_3N are shown in Figure 3. ^{68}Ga-S_3N cleared rapidly from the blood with an initial high liver uptake (72 ± 7 %ID/organ at 2 min) followed by rapid washout (21 ± 1 %ID/organ at 60 min). High uptake was also seen in the lungs (3 ± 1 %ID/organ at 2 min), which accumulated over time (6 ± 1 %ID/organ at 60 min), and the spleen (5 ± 2 %ID/organ at 2 min), which cleared with time (0.25 ± 0.04 %ID/organ at 60 min). Significant uptake was observed in the brain (0.13 ± 0.2 %ID/organ at 2 min), which increased over time to 0.40 ± 0.07 %ID/organ at 60 min, with brain:blood ratios increasing from 0.11 at 2 min postinjection to 3.8 at 60 min postinjection. Uptake was also seen in the heart (1.04 ± 0.26 %ID/organ at 2 min) decreasing to 0.50 ± 0.12 %ID/organ at 60 min, with a heart:blood ratio of 2.5 at 2 min postinjection and 11 at 60 min postinjection.

The biodistribution results in hamsters for ^{68}Ga-S_3N are shown in Figure 4. The complex cleared rapidly from the blood in hamsters as observed in rats; however, the blood values for hamsters (3.5 ± 0.4 %ID/organ at 30 min) at all but the initial timepoints were higher than those observed in rats (1.2 ± 0.1 %ID/organ at 30 min). The high initial liver uptake that was seen for rats was also observed for hamsters (94 ± 11 %ID/organ at 5 min). The washout from the liver, as seen in Figure 5, was significantly slower in hamsters (70 ± 5 %ID/organ at 60 min). The lung uptake in hamsters, as seen in Figure 5, was similar to that observed in rats at the early time point (3 ± 1 % at 5 min); however, uptake did not increase as observed in rats but actually decreased (2.6 ± 0.2 %ID/organ at 60 min). Spleen uptake was high initially (2.2 ± 0.6 %ID/organ at 5 min) but decreased over time (0.11 ± 0.03 %ID/organ at 60 min). Significant uptake was observed in the heart (1.04 ± 0.8 %ID/organ at 5 min), with a heart:blood ratio of 9.9 at 5 min, decreasing over time (0.30 ± 0.08 %ID/organ at 60 min), with a heart:blood ratio of 1.5 comparable to that observed for rats as seen in Figure 5. Significant uptake was observed in the brain (0.13 ± 0.03 %ID/organ at 5 min), with a brain:blood ratio of 0.4 at 5 min, that increased over time (0.25 ± 0.04 %ID/organ at 60 min) to a brain:blood ratio of 0.5 at 60 min; however, as seen in Figure 6, the uptake was lower than that observed in rats.

Autoradiography Studies

The brain distribution in normal rats of ^{68}Ga-S_3N was compared with that of two known blood flow tracers, ^{64}Cu-PTSM and ^{11}C-ethanol. The rats were sacrificed, the brains were removed, sliced, and imaged on an Instant Imager. The images obtained with ^{68}Ga-S_3N, ^{64}Cu-PTSM and ^{11}C-ethanol are shown in Figure 7. The autoradiography scans of ^{68}Ga-S_3N and ^{64}Cu-PTSM were similar. The only notable difference was the higher uptake of ^{68}Ga-S_3N in the cortex in the back of the brain. The scan of brain slices containing ^{11}C-ethanol were notably different than those of ^{68}Ga-S_3N. ^{11}C-ethanol was distributed more evenly or diffusely throughout the brain than ^{68}Ga-S_3N. These results reflect the similar lipophilicities of ^{68}Ga-S_3N and ^{64}Cu-PTSM.

Primate Imaging Study

Figure 8 shows the PET brain images obtained with ^{68}Ga-S_3N and ^{15}O-water. The brain uptake at 1 min postinjection was 3.9 %ID/organ and decreased to 2.4 %ID/organ at 15 min, where it remained until the end of the study. Similar to the autoradiography results in the rat brain, the brain uptake of ^{68}Ga-S_3N showed greater uptake in the cortex at the back of the brain. Higher uptake was also demonstrated in the clivus and the temporal mandibular joints, as demonstrated in Figure 9. Although the reason for this high uptake in the clivus and mandibular joints is not known, it has been observed by us and others for radiopharmaceuticals targeted to specific receptors in the brain (5, 26).

Canine Imaging Studies

Figure 10 shows the heart imaging studies obtained with ^{68}Ga-S_3N and ^{15}O-water. The high lung uptake observed in both rats and hamsters was also observed in canines. The lung uptake as depicted in Figure 11 greatly decreased over time, differing from that observed in either rats or hamsters. The liver uptake remained fairly constant over time, as shown in Figure 11. The liver uptake in both rats and hamsters declined over time. The clearance from the myocardium is shown in Figure 11 and was comparable to that observed in both rats and hamsters.

Molecular Modeling

A molecular mechanics technique referred to as the "coordination scan," which successfully predicts the coordination number of metal complexes, has been used to understand the behavior of Ga(III) and In(III) complexes with a series of multidentate thiolate ligands, EDDASS, 4SS, 5SS, and 6SS (34). The coordination scan, shown in Figure 12, indicated that this ligand would bind Ga(III).

The Ga(III) complex was predicted to be 4-coordinate in a tetrahedral geometry, thus fulfilling the coordination requirements of the metal. This prediction was later confirmed by x-ray crystallography (27).

DISCUSSION

We have described a gallium-labeled complex that is extracted into the brain more than any gallium complex described in the literature thus far. ^{68}Ga-S_3N meets many of the requirements of a potential brain imaging agent: it has a low molecular weight, it is neutral, lipophilic, and stable to transchelation to transferrin. Along with extraction in the brain, ^{68}Ga-S_3N also exhibited significant heart uptake.

Of all the ^{68}Ga agents reported in the literature, only ^{68}Ga-THM_2BED showed uptake in the brain. The neutral lipophilic hexachelated complex ^{68}Ga-THM_2BED was shown to cross the

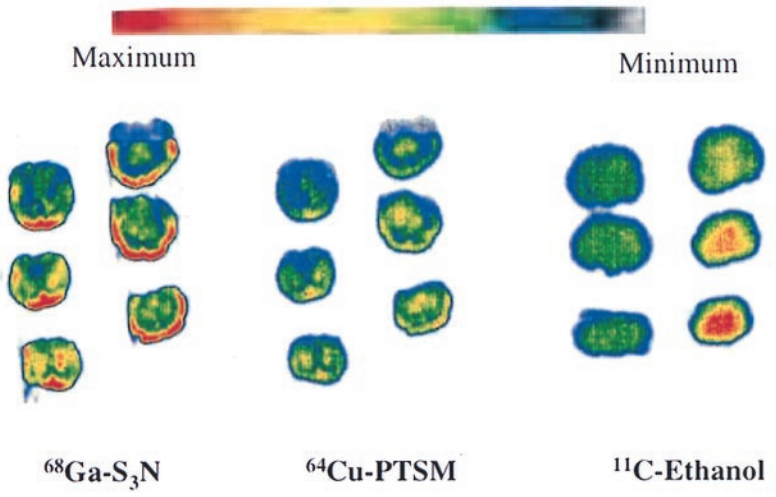

FIG. 7. ***Ex vivo*** **imaging of a normal rat brain. The brain slices on the far left show the distribution of ^{68}Ga-S$_3$N. The brain slices in the middle show the distribution of ^{64}Cu-PTSM. The brain slices on the far right show the distribution of ^{11}C-ethanol.**

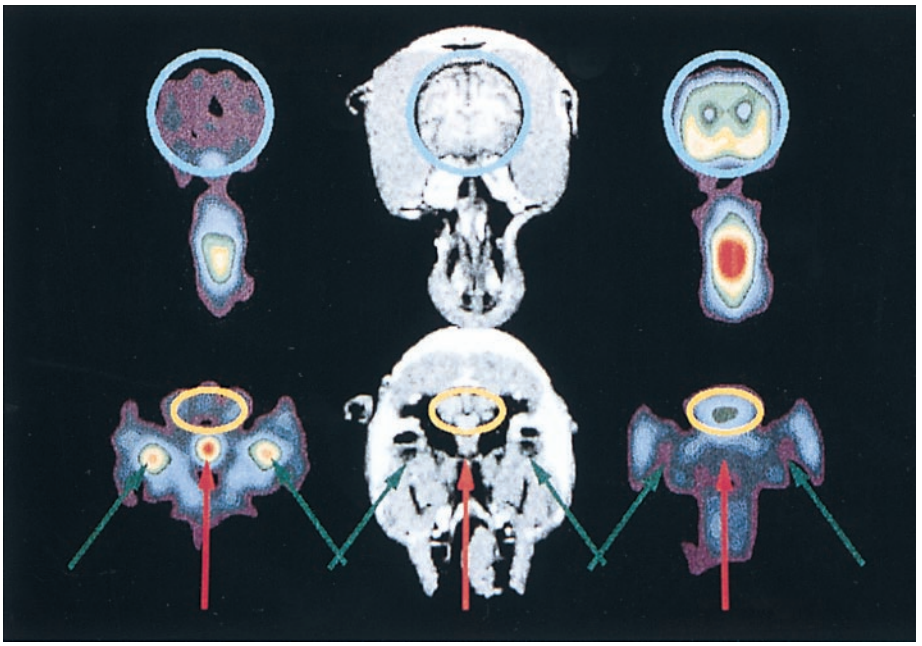

FIG. 8. Magnetic resonance imaging (MRI) and positron emission tomography (PET) coregistry study of ^{68}Ga-S$_3$N in a male Nemestrina macaque. On the far left is shown the distribution of ^{68}Ga-S$_3$N in the brain. In the middle is shown the MRI image of the brain. On the far right is shown the distribution of O-15-labeled water. The arrows point to the clivus and temporal mandibular joints, whereas the circles outline the brain in each image.

(NOTE: FIG. 9 is located on pg. 313)

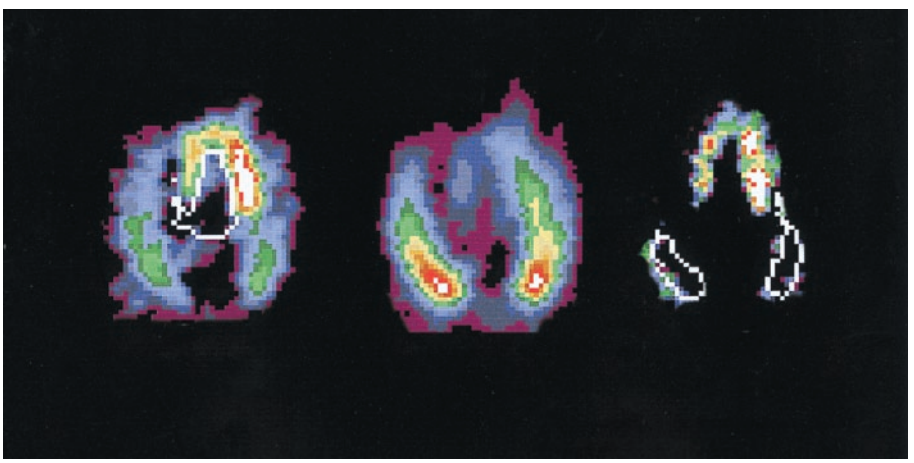

FIG. 10. Reconstructed midventricular positron emission tomography (PET) images of the heart from a normal dog obtained after administration of O-15 water and corrected for blood activity (left) and corresponding midventricular reconstruction obtained after administration of Ga-68 (center), and same Ga-68 reconstruction after correction of tracer uptake in the lungs (right). Note that significant myocardial uptake of Ga-68 occurs in normal myocardium (right). Images are displayed on their horizontal long axis where septum is to the left, anterior-apex is uppermost, and lateral is to the right.

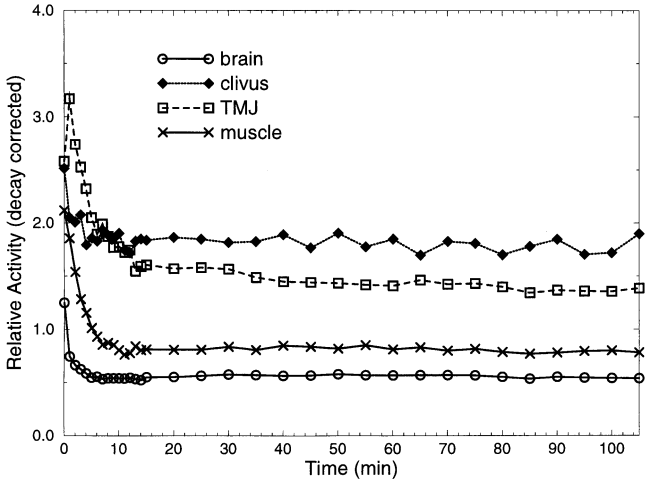

FIG. 9. Plot showing the relative uptake of ^{68}Ga-S_3N in the brain and other regions in the primate (temporal mandibular joints = TMJ, clivus, and muscle). The plotted ordinate values represent decay corrected activity per cc of tissue expressed in arbitrary units.

blood–brain barrier with a brain:blood ratio of 0.071 ± 0.10 at 1 h postinjection, which is significantly lower than that for ^{68}Ga-S_3N (3.8 ± 0.3 at 1 h postinjection) (21). The heart:blood ratio for the hexachelated ^{68}Ga-THM_2BED complex (1.65 ± 0.26 at 1 h postinjection) (21) is much lower than that of ^{68}Ga-S_3N (11.0 ± 0.5 at 1 h postinjection). Listed in Table 1 are tissue uptake values for several Ga agents (10, 19, 21, 38). The heart uptake of Ga-BAT-TECH is initially higher than that observed for ^{68}Ga-S_3N; however, Ga-BAT-TECH clears more quickly from the heart, and by 30 min the heart uptake of ^{68}Ga-S_3N is higher (19). The heart uptake values for ^{68}Ga-S_3N are slightly higher than those reported for ^{68}Ga(5-MeOSal)$_3$TAME (8, 11). ^{67}Ga[(4,6-MeO_2sal)$_2$BAPEN]$^+$, developed by Tsang and co-workers (36, 37), exhibits similar heart uptake to ^{68}Ga-S_3N initially; however, over time the heart uptake of ^{67}Ga[(4,6-MeO_2sal)$_2$BAPEN]$^+$, which does not clear from the heart, is higher than that observed for ^{68}Ga-S_3N.

In vitro serum stability analyzed by both reversed phase and normal phase TLC in rat serum incubated at 37°C, showed the ^{68}Ga-S_3N complex to be more than 95% intact at 2 h. *In vivo*, reversed phase TLC showed that ^{68}Ga-S_3N remains stable long enough to quickly clear from the blood and to prevent transchelation of gallium to serum proteins. By 30 min, the remaining ^{68}Ga activity in the blood consists of three radioactive complexes: the original intact complex and two less lipophilic metabolites.

From the coordination scan, it was predicted that Ga would form a 4-coordinate tetrahedral complex with S_3N. A mix of ^{68}Ga-S_3N complexes with various waters (i.e. 5- and 6-coordinate) is not possible because the energy differences between the 4-coordinate curve and the 5- and 6-coordinate curves are too great. Previous studies showed Ga(III) forms stable complexes with either 4-, 5-, or 6-coordinate ligands, indicating that the 4-coordinate Ga-S_3N complex should be stable (34). Interestingly, the In complex of this ligand is determined to be 5-coordinate. The prediction agrees with the x-ray structure (27).

The pattern of biodistribution for the ^{68}Ga-S_3N complex in rats is especially interesting. The ^{68}Ga-S_3N complex cleared rapidly from the blood, and demonstrated very high liver uptake at early times postinjection that cleared over time. This rapid clearance from the blood and subsequent clearing from the liver suggests this complex is stable to metal transchelation *in vivo*. It has been shown that unstable gallium complexes tend to clear slowly from the blood and accumulate in the liver (17, 22). ^{68}Ga-S_3N had high uptake in the lungs that increased over time, and had somewhat high uptake in the spleen that cleared over time. The brain distribution of ^{68}Ga-S_3N, as shown by autoradiography, is that expected of a lipophilic agent. The brain distribution was similar to ^{64}Cu-PTSM in the normal rat and primate, but exhibited higher uptake in the

TABLE 1. Biodistribution Data of Various Ga Agents in Rats

	Time from injection (min)				
Compound	**2**	**5**	**15**	**30**	**60**
Blood					
^{68}Ga-S_3N	8.51 ± 1.88		0.98 ± 0.21	1.18 ± 0.13	0.76 ± 0.17
^{68}Ga[(4,6-MeO_2sal)$_2$Bapen]$^+$		1.54 ± 0.18	0.96 ± 0.04	0.63 ± 0.02	0.43 ± 0.04
^{67}Ga-BAT-TECH	10.18 ± 0.30			3.58 ± 0.08	4.54 ± 1.10
^{68}Ga-THM_2BED		11.30 ± 8.071		10.13 ± 1.089	5.767 ± 1.333
^{67}Ga-[(5-MeOsal)$_3$tame-O-*n*-Pr		4.03 ± 0.29			1.51 ± 0.09
Heart					
^{68}Ga-S_3N	1.04 ± 0.26		0.77 ± 0.19	0.95 ± 0.14	0.49 ± 0.13
^{68}Ga-[4,6-MeO_2sal)$_2$Bapen]$^+$		1.08 ± 0.15	0.87 ± 0.10	0.87 ± 0.10	1.02 ± 0.09
^{67}Ga-BAT-TECH	1.68 ± 0.12			0.52 ± 0.08	0.26 ± 0.02
^{68}Ga-THM_2BED		1.135 ± 0.170		0.686 ± 0.354	0.500 ± 0.058
^{67}Ga-[(5-MeOsal)$_3$tame-O-*n*-Pr		0.70 ± 0.05			0.22 ± 0.03
Brain					
^{68}Ga-S_3N	0.13 ± 0.03		0.25 ± 0.04	0.42 ± 0.05	0.40 ± 0.07
^{68}Ga-[4,6-MeO_2sal)$_2$Bapen]$^+$		0.02 ± 0.01	0.01 ± 0.01	0.01 ± 0.01	0.01 ± 0.01
^{67}Ga-BAT-TECH	0.02 ± 0.004			0.01 ± 0.001	0.01 ± 0.002
^{68}Ga-THM_2BED		0.090 ± 0.020		0.084 ± 0.015	0.056 ± 0.010
^{67}Ga-[5-MeOsal)$_3$tame-O-*n*-Pr		0.02 ± 0.002			0.015 ± 0.002

Values presented as % injected dose/organ (±SD).

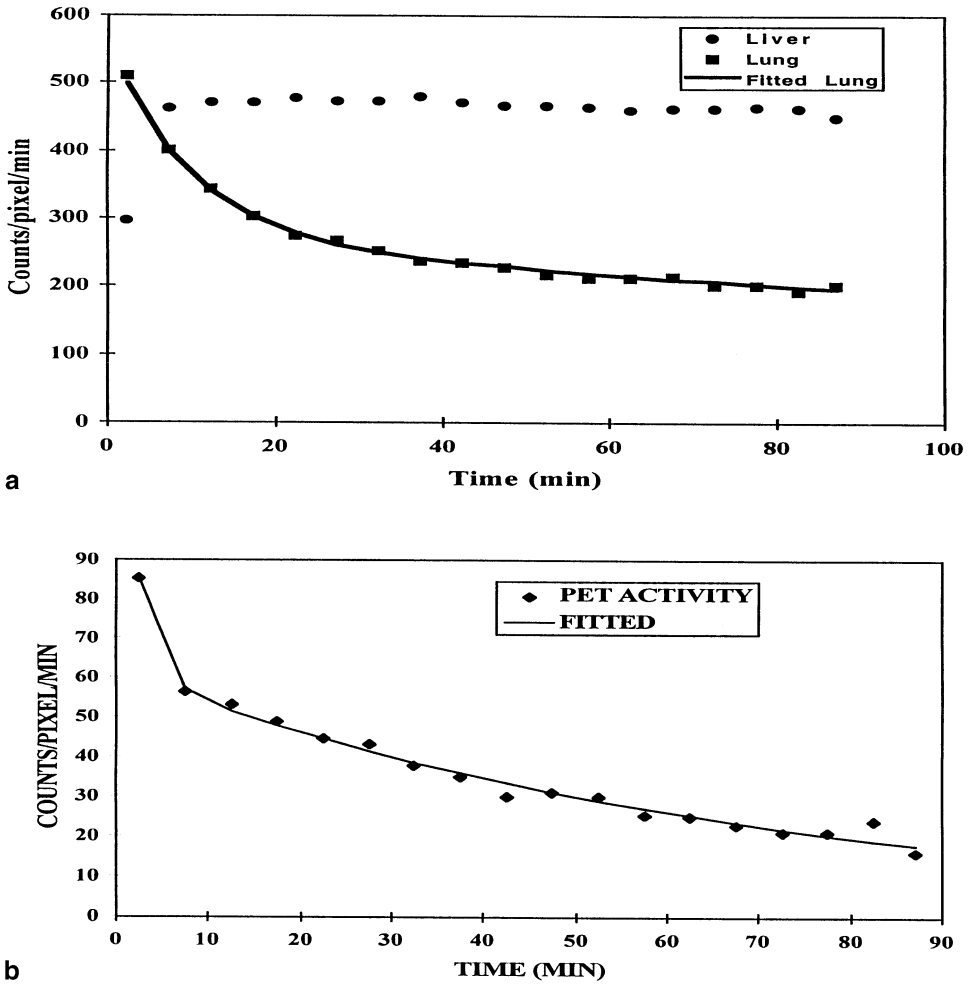

FIG. 11. Positron emission tomography (PET) Ga-68 time–activity curves obtained in a normal dog from liver and lungs (a), and heart (b). Note that there is significantly greater uptake of tracer in the liver and lungs when compared with the heart, and that whereas Ga-68 starts clearing from the lungs and heart within the first few minutes after injection of tracer, it is retained by the liver.

back cortex of the brain. Studies are ongoing at this time to determine what is responsible for this anomalous brain uptake.

A comparison of the uptake of ^{68}Ga-S_3N in rat, hamster, and dog models shows very different lung and liver uptake and clearance. In rats, ^{68}Ga-S_3N clears rapidly from the liver and accumulates in the lung over time, whereas the reverse was observed in dogs. In, hamsters the lung and liver uptake decreased slowly over time. Heart uptake for all three species was similar, as shown in Figures 5 and 11. Although the heart can be seen as shown in Figure 11, the image is less than optimal due to the high liver and lung uptake. We are currently investigating altering the structure of S_3N to improve the clearance of activity from the lung and liver, thereby improving its myocardial imaging. Brain uptake was higher in the rat (0.42 %ID/organ at 30 min postinjection) than in the hamster (0.23 %ID/organ at 30 min postinjection) (Fig. 6). However, the highest brain uptake was observed in the primate, 2.4 %ID/organ at 30 min postinjection. A species dependence was also observed for a series of Ga(III) tris(1-aryl-3-hydroxy-2-methyl-4-pyridinato) complexes developed as potential myocardial agents (39). The ^{67}Ga-labeled series of compounds were evaluated in rat, dog, mice, and hamster models. In rabbits and dogs, the complexes showed rapid heart uptake and blood clearance, whereas in rats and mice the blood clearance was very slow. One complex in particular, 3-hydroxy-2-methyl-1-(p-nitrophenyl)-4-pyridinone labeled with Ga(III), showed accumulation in the brain of normal rabbits that increased over time (39). This brain uptake was not observed in any of the other animal models. In a more elaborate study denoted as "The Noah's Ark Experiment," ^{99m}Tc cationic complexes developed as myocardial imaging agents were evaluated in 10 different animal species (3). The ^{99m}Tc cationic compounds showed different biodistribution patterns that were species dependent. None of these animal models adequately predicted the behavior of these compounds in humans. The imaging was either far better or far worse than that observed in humans (3). Based on the species dependence of ^{68}Ga-S_3N, human studies will be necessary to determine its behavior. ^{68}Ga-S_3N in rats and hamsters behaves atypically of other perfusion agents in that the brain uptake is not first pass but accumulates over time, as demonstrated in Figure 6. Normally, a perfusion agent exhibits its highest uptake in the organ of interest immediately postinjection when the agent's concentration is highest in the blood. The high lung uptake and retention is also interesting. Possible explanations for the gradual increase in brain uptake of ^{68}Ga-S_3N over time include: re-extraction of ^{68}Ga-S_3N into the brain and lung after originally being taken up by other

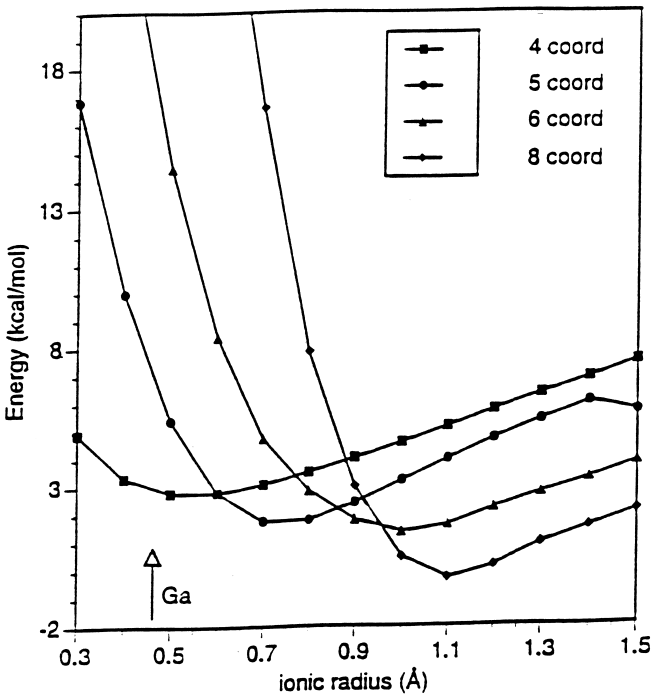

FIG. 12. Coordination scan of ^{68}Ga-S_3N indicating the relative energies of the various coordination states. The Ga(III) ionic radius (0.47 Å) of the preferred four coordinate complex is indicated by an arrow.

tissues such as the liver and then released, or metabolism of ^{68}Ga-S_3N in the liver forming a compound that is able to cross the blood–brain barrier. Preliminary metabolism studies in rats show that ^{68}Ga-S_3N is metabolized in the liver, forming three less lipophilic metabolites.

CONCLUSIONS

In conclusion, S_3N was successfully labeled with Ga. The biodistribution of the Ga S_3N complex showed it was taken up rapidly by the liver and exhibited significant uptake in the heart and brain. Molecular mechanics calculations predicted that Ga-S_3N was kinetically stable. The high brain uptake of ^{68}Ga-S_3N was also observed in a nonhuman primate, demonstrating the potential for this agent as a diagnostic PET tracer for cerebral blood flow.

We thank Carmen Dence for synthesizing ^{11}C-ethanol. This work was funded by DOE grant no. DE-FG02-87ER60512.

References

1. Anderson C. J., John C. S., Li Y. J., Hancock R. D., McCarthy T. J., Martell A. E. and Welch M. J. (1995) *N,N′*-ethylene-di-L-cysteine (EC) complexes of Ga(III) and In(III): Molecular modeling, thermodynamic stability and in vivo studies. *Nucl. Med. Biol.* **22,** 165–173.
2. Anderson C. J. and Welch M. J. (1994) Gallium. In: *Handbook on metals in clinical and analytical chemistry* (Edited by Seiler H. G., Sigel A. and Sigel H.), pp. 371–380. Marcel Dekker, Inc., Basel, Switzerland.
3. Deutsch E. A., Ketring A. R., Libson K., Vanderheyden J. L. and Hirth W. W. (1989) The Noah's ark experiment: Species dependent biodistributions of cationic ^{99m}Tc complexes. *Int. J. Radiat. Appl. Instrum., Part B Nucl. Med. Biol.* **16,** 191–232.
4. Dischino D. D., Welch M. J., Kilbourn M. R. and Raichle M. R. (1983) Relationship between lipophilicity and brain extraction of C-11-labeled radiopharmaceuticals. *J. Nucl. Med.* **24,** 1031–1038.
5. Eberling J. L., Enas J. D. and Budinger T. F. (1998) The misidentification of midbrain anatomical structures using neurochemical imaging. *J. Nucl. Med.* **39,** 208.
6. Francesconi L. C., Liu B. L., Billings J. J., Carroll P. J., Graczyk G. and Kung H. F. (1991) Synthesis, characterization and solid state structure of a neutral gallium(III) amino thiolate complex: A potential radiopharmaceutical for PET imaging. *J. Chem. Soc., Chem. Commun.* **2,** 94–95.
7. Govindaswamy N., Quarless D. A. Jr. and Koch S. A. (1995) New amine trithiolate tripod ligand and its iron(II) and iron(III) complexes. *J. Am. Chem. Soc.* **117,** 8468–8469.
8. Green M. A. (1986) Synthesis and biodistribution of a series of lipophilic gallium-67 tris(salicylaldimine) complexes. *J. Labelled Compd. Radiopharm.* **23,** 1227–1229.
9. Green M. A. (1987) Potential copper radiopharmaceutical for imaging the heart and brain: Copper-labeled pyruvaldehyde bis(N^4-methylthiosemicarbazone). *Nucl. Med. Biol.* **14,** 59–61.
10. Green M. A., Mathias C. J., Neumann W. A., Fanwick P. E., Janik M. and Deutsch E. A. (1993) Potential gallium-68 tracers for imaging the heart with PET: Evaluation of four gallium complexes with functionalized tripodal tris(salicylaldimine) ligands. *J. Nucl. Med.* **34,** 228–233.
11. Green M. A., Welch M. J., Mathias C. J. Fox K. A. A., Knabb R. M. and Huffman J. C. (1985) Gallium-68 1,1,1-tris(5-methoxysalicylaldiminomethyl)ethane: A potential tracer for evaluation of regional myocardial blood flow. *J. Nucl. Med.* **26,** 170–180.
12. Hack S. N., Eichling J. O., Bergmann S. R., Welch M. J. and Sobel B. E. (1980) External quantification of myocardial perfusion by exponential infusion of positron-emitting radionuclides. *J. Clin. Invest.* **66,** 918–927.
13. Hancock R. D. (1986) Macrocycles and their selectivity for metal ions on the basis of size. *Pure Appl. Chem.* **58,** 1445–1452.
14. Hancock R. D. (1989) Molecular mechanics calculations as a tool in coordination chemistry. *Prog. Inorg. Chem.* **37,** 187–291.
15. Hancock R. D. (1990) Molecular mechanics calculations and metal ion recognition. *Acc. Chem. Res.* **23,** 253–257.
16. Hancock R. D., Reichert D. E. and Welch M. J. (1996) Molecular mechanics force field for modeling technetium(V) complexes. *Inorg. Chem.* **35,** 2165–2166.
17. Harris W. R. and Pecoraro V. L. (1983) Thermodynamic binding constants for gallium transferrin. *Biochemistry* **22,** 292–299.
18. Hegetschweiler K., Hancock R. D., Ghisletta M., Kradolfer T., Gramlich V. and Schmalle H. W. (1993) 1,3,5-trideoxy-*cis*-inositol, a ligand with a remarkable versatility for metal ions. 5. Complex formation with magnesium(II), calcium(II), strontium(II), barium(II) and cadmium(II). *Inorg. Chem.* **32,** 5273–5284.
19. Kung H. F., Liu B.-L., Billings J. J., Francesconi L. C. and Alavi A. (1990) A new myocardial imaging agent: Synthesis, characterization and biodistribution of gallium-68-BAT-TECH. *J. Nucl. Med.* **31,** 1635–1640.
20. Loc'h C., Maziere B. and Comar D. (1980) A new generator for ionic gallium-68. *J. Nucl. Med.* **21,** 171–173.
21. Madsen S. L., Welch M. J., Motekaitis R. J. and Martell A. E. (1992) ^{68}Ga-THM_2BED: A potential generator-produced tracer of myocardial perfusion for positron emission tomography. *Int. J. Radiat. Appl. Instrum., Part B Nucl. Med. Biol.* **19,** 431–44.
22. Mathias C. J., Sun Y. Z., Welch M. J., Green M. A., Thomas J. A., Wade K. R. and Martell A. R. (1988) Targeting radiopharmaceuticals: Comparative biodistribution studies of gallium and indium complexes of multidentate ligands. *Int. J. Radiat. Appl. Instrum., Part B Nucl. Med. Biol.* **15,** 69–81.
23. Matsumoto K., Fujibayashi Y., Yonekura Y., Wada K., Takemura Y., Konishi J. and Yokoyama A. (1992) Application of the zinc-62/copper-62 generator: An effective labeling method for Cu-62-PTSM. *Nucl. Med. Biol.* **19,** 39–44.
24. Mazoyer B., Trebossen R., Deutch R., Casey M. and Blohm K. (1991) Physical characteristics of the ECAT 953B/31: A new high resolution brain positron tomograph. *IEEE Trans. Med. Imag.* **10,** 499–504.
25. McCarthy D. W., Shefer R. E., Klinkowstein R. E., Bass L. A., Margenau W. H., Cutler C. S., Anderson C. J. and Welch M. J. (1997) Efficient production of high specific activity ^{64}Cu using a biomedical cyclotron. *Nucl. Med. Biol.* **24,** 35–43.
26. McCarthy T. J., Sherman E. L. C., Talley J. J., Seibert K., Isakson P. C. and Welch M. J. (1995) Radiosynthesis, biodistribution and PET

imaging of potent and selective inhibitors of cyclooxygenase-1 and cyclooxygenase-2. *J. Nucl. Med.* **36,** 49P.
27. Motekaitis R. J., Martell A. E., Koch S. A., Hwang J. W., Quarless D. A. and Welch M. J. (1998) The gallium (III) and indium(III) complexes of tris(2-mercaptobenzyl)amine and tris(2-hydroxybenzyl)amine. *Inorg Chem.* **37,** 5902–5911.
28. Reichert D. E., Hancock R. D. and Welch M. J. (1996) Molecular mechanics investigation of gadolinium(III) complexes. *Inorg. Chem.* **35,** 7013–7020.
29. Shannon R. D. (1976) Revised effective ionic radii and systematic studies of interatomic distances in halides and chalcogenides. *Acta Crystallogr., Sect. A: Found. Crystallogr.* **32,** 751–767.
30. Shelton M. E., Green M. A., Mathias C. J., Welch M. J. and Bergmann S. R. (1989) Kinetics of copper-PTSM in isolated hearts: A novel tracer for measuring blood flow with positron emission tomography. *J. Nucl. Med.* **30,** 1843–1847.
31. Shelton M. E., Green M. A., Mathias C. J., Welch M. J. and Bergmann S. R. (1990) Assessment of regional myocardial and renal blood flow with copper-PTSM and positron emission tomography. *Circulation* **82,** 990–997.
32. Spinks T., Jones T., Bailey D., Townsend D., Grootoonk S., Bloomfield P., Gilardi M., Casey M., Sipe B. and Reed J. (1993) Physical performance of positron tomograph for brain imaging with retractable septa. *Phys. Med. Biol.* **37,** 1637–1655.
33. Spinks T. J., Jones T., Gilardi M. C. and Heather J. D. (1988) Physical performance of the latest generation of commercial positron scanner. *IEEE Trans. Nucl. Sci.* **35,** 721–725.
34. Sun Y., Anderson C. J., Pajeau T. S., Reichert D. E., Hancock R. D., Motekaitis R. J., Martell A. E. and Welch M. J. (1996) Indium (III) and Gallium(III) complexes of bis(aminoethanethiol) ligands with different denticities: Stabilities, molecular modeling and *in vivo* behavior. *J. Med. Chem.* **39,** 458–470.
35. Thöm V., Fox C. C., Boeyens J. C. A. and Hancock R. D. (1984) Molecular mechanics and crystallographic study of hole sizes in nitrogen-donor tetraaza macrocycles. *J. Am. Chem. Soc.* **106,** 5947–5955.
36. Tsang B. W., Mathias C. J., Fanwick P. E. and Green M. A. (1994) Structure–distribution relationships for metal-labeled myocardial imaging agents: Comparison of a series of cationic gallium(III) complexes with hexadentate bis(salicylaldimine) ligands. *J. Med. Chem.* **37,** 4400–4406.
37. Tsang B. W., Mathias C. J. and Green M. A. (1993) A gallium-68 radiopharmaceutical that is retained in myocardium: ^{68}Ga[4,6-Me_2sal]$_2$BAPEN]$^+$. *J. Nucl. Med.* **34,** 1127–1131.
38. *Tripos SYBYL*, 6.2 ed. (1995) Tripos Inc., St. Louis, MO.
39. Zhang Z., Lyster D. M., Webb G. A. and Orvig C. (1992) Potential ^{67}Ga radiopharmaceuticals for myocardial imaging: Tris(1-aryl-3-hydroxy-2-methyl-4-pyridinato)gallium(III) complexes. *Nucl. Med. Biol.* **19,** 327–335.